Determination of Judd–Ofelt intensity parameters from the excitation spectra for rare-earth doped luminescent materials

Wenqin Luo,[ab] Jinsheng Liao,[ab] Renfu Li[ab] and Xueyuan Chen*[ab]

Received 15th October 2009, Accepted 14th January 2010
First published as an Advance Article on the web 10th February 2010
DOI: 10.1039/b921581f

By utilizing the proportional relationship between the excitation and absorption spectra for some special excited multiplets of rare-earth (RE) ions that are followed by a very fast nonradiative relaxation to the monitored level, we propose a new approach to determine the Judd–Ofelt (JO) intensity parameters that are crucial to the evaluation of laser and luminescent materials *via* excitation spectra. To validate this approach, the JO parameters of $NaGd(WO_4)_2:Er^{3+}$ and $YLiF_4:Nd^{3+}$ crystals are calculated and compared through both the excitation and absorption spectra. The JO parameters derived from this approach are in good agreement with that determined from the conventional method (absorption spectra). Furthermore, the JO intensity parameters of $Y_2O_3:Er^{3+}$ nanocrystals are derived from the excitation spectra by taking into account the nano-size effects, which are comparable to the values of the crystal counterpart. The proposed approach is of particular importance for those powders or nanophosphors with low RE doping concentration that their quantitative absorption spectra are difficult to measure.

1. Introduction

Rare-earth (RE) ions doped materials have been widely used for solid-state lasers, lighting and displays, optical communications, fluorescent biolabels, and other photonic devices.[1–17] Judd–Ofelt (JO) intensity parameters, in terms of Ω_t ($t = 2, 4, 6$), are crucial to evaluating the performance of the laser and luminescent materials.[18–20] Generally, the three JO intensity parameters are determined empirically from the room temperature (RT) absorption spectrum by minimizing the differences between the calculated and the experimental transition line (or oscillator) strengths of a series of excited multiplets by standard least-squares or chi-square methods.[18,20] Once the JO parameters are obtained, the spontaneous emission probabilities, the oscillator strength, and the radiative branching ratios between J-multiplets of RE ions can be estimated. Typically, the Ω_2 parameter is associated with short-range coordination effects. The higher polarization and asymmetry of the RE ligands, the larger Ω_2 value is expected. Nevertheless, the other two parameters $\Omega_{4,6}$ depend on long-range effects.[20] So far, this conventional method has been extensively and effectively used in the optical characterization of RE doped single crystals, polycrystalline, glasses, and solutions since 1962.[20] However, it meets great limitation in the calculation of JO parameters of nanomaterials in form of powders since the quantitative absorption spectra of these materials can hardly be measured especially for the case of low RE dopant concentration. Nowadays with the development of novel nanophosphors, it is urgent to find more convenient methods for the determination of JO intensity parameters for powders or nanocrystalline materials, which are essential to predicting RE spectral properties for a variety of material applications. A method for direct calculation of JO intensity parameters of Eu^{3+} through emission spectra was proposed by Krupke, taking advantage of the fact that the intensities of the $^5D_0$–$^7F_2$, $^5D_0$–$^7F_4$, and $^5D_0$–$^7F_6$ transitions are solely dependent on the Ω_2, Ω_4, and Ω_6 parameters, respectively,[21] which has been recently applied in various Eu^{3+} doped nanophosphors.[22,23] In addition, the JO intensity parameters of Gd^{3+} in YOCl powders were also derived from the emission spectra and the radiative decay measurement by J. Sytsma and coworkers.[24] However, to date, an approach simply based on the measurement of the excitation spectra has not been proposed to determine the JO parameters for RE^{3+} ions doped powders or nanocrystals.

In this work, we provide a new way for the calculation of JO intensity parameters based on the RT excitation spectra. To validate this approach, we apply it to the determination of JO parameters of two model systems: $NaGd(WO_4)_2:Er^{3+}$ (NGW:Er) and $YLiF_4:Nd^{3+}$ (YLF:Nd) crystals. The results are compared with that calculated by the conventional method through the absorption spectra. Finally, to exemplify its usefulness in nanophosphors, the approach is introduced to determine the JO parameters of $Y_2O_3:Er^{3+}$ nanocrystals.

2. Theoretical considerations

To some extent, the corrected excitation spectrum can be regarded as a part of the absorption spectrum that was used to emit light from the monitored levels. The difference between the excitation and absorption spectra mainly lies in the relative fluorescence efficiency, that is, the intensity ratio of the fluorescence excitation to the absorption.[25] If the relative

[a] *Key Laboratory of Optoelectronic Materials Chemistry and Physics, Fujian Institute of Research on the Structure of Matter, Chinese Academy of Sciences, Fuzhou, Fujian 350002, China. E-mail: xchen@fjirsm.ac.cn; Fax: +86591 8764-2575; Tel: +86 5918764-2575*
[b] *State Key Laboratory of Structural Chemistry, Fuzhou, Fujian 350002, China*

fluorescence efficiency keeps constant at different wavelengths, the excitation spectrum can therefore coincide exactly with the absorption spectrum. It has been turned out that the excitation spectrum reproduces well the corresponding absorption spectrum for the excitation to those levels that are followed by a very fast nonradiative relaxation to the monitored level.[26,27] As a matter of fact, this is equivalent to a special situation discussed by Partlow and Moos, in which the quantum efficiency η_{AB} from an excited level (A) to its low-lying level (B) is assumed to be 1.[28] The applicable monitored levels and the excited states of different RE^{3+} ions that meet the prerequisite (namely, excited multiplets should nonradiatively relax to the monitored level very fast) were summarized in Table 1. For instance, for Er^{3+} ions, those excited multiplets of $^2H_{11/2}$, $^4F_{7/2}$, $^4F_{5/2}$, and $^4F_{3/2}$ when monitoring the emission from the metastable $^4S_{3/2}$ may satisfy the above condition, and thus could be selected as ideal J-multiplets for the proposed JO parameters determination. Similarly, the target multiplets in the excitation may be $^2H_{11/2}$, $^4F_{9/2}$, $^4F_{7/2}$, $^4S_{3/2}$, $^4F_{5/2}$ and $^2H_{9/2}$ when monitoring the emission from $^4F_{3/2}$ for Nd^{3+} ions. The energy levels of Er^{3+} and Nd^{3+} ions are schematically plotted in Fig. 1. The above proportionality between the absorption and excitation spectra is then utilized to perform the following JO calculation.

The measured line strengths S_{mea} are calculated from the excitation spectrum by:

$$S_{mea}(J \rightarrow J') = \frac{C}{\bar{\lambda}} \frac{9n}{(n^2+2)^2} \Gamma_{exc} \qquad (1)$$

where J (J') is the angular momentum quantum number of the initial (final) state (for Er^{3+} $J = 15/2$; for Nd^{3+} $J = 9/2$); C is a proportional constant that includes the calibration factor for the optical detecting system; n is the refractive index of the sample. In case of nanocrystals, n should be replaced by an effective index of refraction n_{eff} considering the filling factor x occupied by nanocrystals as will be discussed in the following;[29] and λ is the mean wavelength of the excitation band; Γ_{exc}, a quantity similar to the integrated absorbance for the absorption spectrum, is the integrated excitation intensity for each band

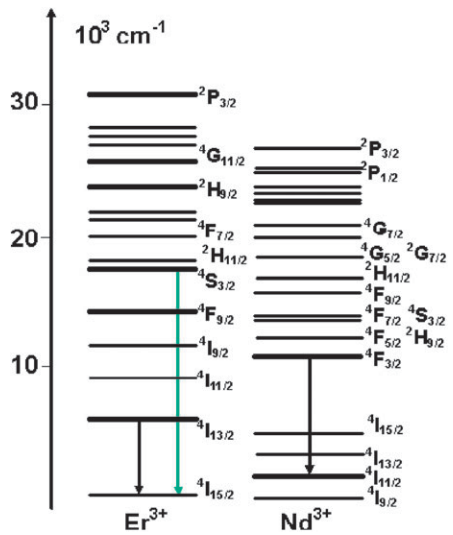

Fig. 1 Schematic energy levels of Er^{3+} and Nd^{3+} ions.

from the initial state to the final state. Note the difference between eqn (1) and the commonly used expression for S_{mea}.[21,26,30] Relative values of S_{mea} (each having a common factor of C), instead of absolute ones for the conventional method, is calculated by eqn (1). The line strengths of optical spectra of RE^{3+} ions in luminescent materials are mainly determined by electric-dipole (ED) and magnetic-dipole (MD) transitions. According to JO theory, the absorption/excitation line strength for an ED transition can also be expressed in terms of $\Omega_{2,4,6}$ parameters by[30]

$$S_{cal}(J \rightarrow J') = \sum_{t=2,4,6} \Omega_t |\langle \Phi J || U^{(t)} || \Phi' J' \rangle|^2 \qquad (2)$$

The reduced matrix elements (RMEs) of the unit tensor $|\langle \Phi J \| U^{(t)} \| \Phi' J' \rangle|$ are adopted from ref. 31 and 32. By a least-squares fitting of S_{cal} to the measured line strengths S_{mea}, the ratios of the three JO intensity parameters $\Omega_{2,4,6}$ can be obtained.

For the emission spectra, the radiative transition rates of the ED and MD transitions from an initial state J to a lower state J' can be calculated according to:

$$A(J \rightarrow J') = \frac{64\pi^4 e^2}{3h(2J+1)\bar{\lambda}^3} \cdot \left[\chi_{ED} \sum_{t=2,4,6} \Omega_t |\langle \Phi J || U^{(t)} || \Phi' J' \rangle|^2 + \chi_{MD} |\langle \Phi J || M || \Phi' J' \rangle|^2 \right] \qquad (3)$$

$$\tau_r^{-1} = \sum_{J'} A(J \rightarrow J') \qquad (4)$$

where $M = -eh(L + 2S)/2mc$ is the MD moment for transition from J to J' and the RMEs of M depend on the free-ion Hamiltonian;[33] τ_r is the radiative lifetime of the emitting multiplet (J); χ_{ED} is the correction factor of the refractive index (n) for an ED transition with $\chi_{ED} = n(n^2+2)^2/9$; χ_{MD} is the correction factor of the refractive index for a MD transition with $\chi_{MD} = n^3$. As shown in eqn (3) and (4), the radiative lifetime depends explicitly on the refractive index of the host. For nanocrystals with a size much smaller than the wavelength of light, n should be replaced by an effective index of refraction (n_{eff}) since only a fraction of the total volume is occupied by nanocrystals.[29] The n_{eff} is defined as: $n_{eff} = n(\lambda)_{np} \cdot x + (1-x) n_{med}$, where x is the filling factor showing what fraction of space is occupied by the nanoparticles with the refractive index of $n(\lambda)_{np}$, and n_{med} is the refractive index of surrounding media.[29] Moreover, for Er^{3+} ions, the measured RT lifetime of $^4I_{13/2}$ by monitoring the $^4I_{13/2} \rightarrow {}^4I_{15/2}$ transition was used as a standard to determine the absolute values of $\Omega_{2,4,6}$ parameters according to eqn (3) and (4). Here, we assume that the quantum efficiency of $^4I_{13/2}$ approaches 1, in view of the large energy gap between $^4I_{13/2}$ and $^4I_{15/2}$ ($\sim 6500\ cm^{-1}$). It should be noted that the corresponding MD contribution was subtracted from the total radiative rate of the $^4I_{13/2} \rightarrow {}^4I_{15/2}$ transition (*i.e.*, inverse of the measured lifetime) in the calculation. Similarly, for Nd^{3+} ions, the measured RT lifetime of $^4F_{3/2}$ by monitoring the $^4F_{3/2} \rightarrow {}^4I_{11/2}$ transition was used as a standard

Table 1 The excited multiplets of different RE^{3+} ions that can be used in the calculation of JO parameters through the excitation spectra

RE^{3+}	Monitored multiplet	Applicable multiplets
Pr^{3+}	$^1P_0$	$^3P_1$, $^1I_6$, $^3P_2$
Nd^{3+}	$^4F_{3/2}$	$^4F_{5/2}$ + $^2H_{9/2}$, $^4S_{3/2}$ + $^4F_{7/2}$, $^4F_{9/2}$, $^2H_{11/2}$, $^2G_{7/2}$ + $^4G_{5/2}$, $^4G_{7/2}$ + $^4G_{9/2}$ + $^2K_{13/2}$, $^4G_{11/2}$ + $^2G_{9/2}$ + $^2D_{3/2}$ + $^2K_{15/2}$, $^2P_{1/2}$ + $^2D_{5/2}$, $^4D_{3/2}$ + $^4D_{5/2}$ + $^2I_{11/2}$ + $^4D_{1/2}$ + $^2L_{15/2}$
Pm^{3+}	$^5F_1$	$^5F_2$, $^5F_3$, $^5S_2$, $^5F_4$, $^5F_5$, $^3H_4$, $^5G_2$, $^5G_3$
Sm^{3+}	$^4G_{5/2}$	$^4F_{3/2}$, $^4G_{7/2}$, $^4I_{9/2}$, $^4I_{13/2}$, $^4F_{5/2}$, $^4M_{17/2}$, $^4M_{19/2}$
Gd^{3+}	$^6P_{7/2}$	$^6P_{3/2}$, $^6P_{5/2}$
Tb^{3+}	$^5D_3$	$^5L_{10}$, $^5G_6$, $^5L_9$, $^5G_5$, $^5D_2$, $^5L_8$, $^5G_4$, $^5L_7$, $^5L_6$, $^5G_3$, $^5G_2$
Dy^{3+}	$^4F_{9/2}$	$^4I_{15/2}$, $^4G_{11/2}$, $^4I_{13/2}$, $^4K_{17/2}$, $^4I_{17/2}$, $^4M_{19/2}$, $^4P_{3/2}$, $^6P_{3/2}$, $^6P_{5/2}$, $^4I_{11/2}$
Ho^{3+}	$^5F_3$	$^5F_2$, $^3K_8$, $^5F_1$
Er^{3+}	$^4S_{3/2}$	$^2H_{11/2}$, $^4F_{7/2}$, $^4F_{5/2}$, $^4F_{3/2}$, $^2H_{9/2}$, $^4G_{11/2}$, $^4G_{9/2}$ + $^2K_{15/2}$ + $^2G_{7/2}$
Tm^{3+}	$^3P_0$	$^3P_1$, $^1I_6$, $^3P_2$

to determine the absolute values of $\Omega_{2,4,6}$ parameters. The MD contribution for the $^4F_{3/2} \rightarrow {}^4I_{11/2}$ transition is zero. Once the absolute values of JO intensity parameters are determined, the line strengths of the ED transition, S_{mea} and S_{cal}, can readily be calculated by eqn (1) and (2), respectively. The root mean square (rms) deviation between the experimental and calculated line strengths is defined as:

$$\mathrm{rms}\Delta\ S = \sqrt{\sum_{i=1}^{N} (S_{mea} - S_{cal})^2 \Big/ (N-3)} \qquad (5)$$

where N is the number of experimental bands involved in the above calculation. The magnitude of the rmsΔS reflects the goodness of the JO parameters fitting.

3. Experimental

The NGW:Er^{3+} (0.75 at.%) crystal and YLF:Nd^{3+} (1 at.%) crystal used in this study were grown by the Czochraski method. The polarized absorption spectra of NGW:Er^{3+} crystal were reported elsewhere.[34] For photoluminescence (PL) and PL excitation characterizations, the crystals were crushed into fine powders.

The Y_2O_3:Er^{3+} (1 at.%) nanocrystals was prepared by a sol–gel combustion method. In detail, 3.83 g $Y(NO_3)_3{\cdot}6H_2O$, 0.047 g $Er(NO_3)_3{\cdot}6H_2O$, 2.54 g citric acid and 2.25 g glycine were dissolved in 10 mL distilled water and 4 mL glycol solution. After 30 min of stirring, the transparent solution was kept at 80 °C for 1 h to afford the sol. The sol was then baked at 100 °C for 12 h to obtain transparent yellow gel. After cooling to RT, the gel was heat treated to 200 °C for 4 h and then 850 °C for 2 h to yield final products.

The absorption spectra of the samples from 200 to 900 nm were recorded with a Perkin-Elmer UV-VIS-NIR spectrometer (Lambda-900). Powder X-ray diffraction (XRD) patterns were collected using a PANalytical X'Pert PRO powder diffractometer with Cu-Kα_1 radiation (λ = 0.154 nm). The morphology of the samples was characterized by a JEOL-2010 transmission electron microscope (TEM). The excitation and emission spectra and luminescence decay curves were recorded on an Edinburgh Instruments FLS920 spectrofluorimeter equipped with continuous (450W) xenon and pulsed xenon (microsecond) lamps. The line intensities of the measured excitation spectra were calibrated for the wavelength dependence of the instrument response including the intensity of the xenon lamp, the transmission efficiency of monochromators, and the quantum efficiency of detector.

4. Results and discussion

4.1 NGW:Er

For Er^{3+} ion doped systems, the NGW:Er crystal was selected as an example for the calculation of JO parameters, because the maximum phonon energy of the $(WO_4)^{2-}$ group is about 900 cm^{-1},[35] and it requires at least 7 phonons to bridge the energy gap between $^4I_{13/2}$ and $^4I_{15/2}$. In order to eliminate the effect of radiation trapping,[36] the luminescence lifetime of $^4I_{13/2}$ of NGW:Er powders (4.07 ms) instead of bulk crystal (4.88 ms)[34] was adopted in the following calculation. Fig. 2 compares the RT excitation and absorption spectra of NGW:Er powders or crystal. It can be seen that the excitation spectrum reproduces well the absorption spectrum in the peak positions and the line intensities. The significant difference below 350 nm is due to the ultraviolet absorption of the host in the absorption spectrum. Seven bands in the RT excitation spectrum, which correspond to the multiplets of $^2H_{11/2}$, $^4F_{7/2}$, $^4F_{5/2}$, $^4F_{3/2}$, $^2H_{9/2}$, $^4G_{11/2}$, and $^4G_{9/2}$ + $^2K_{15/2}$ + $^2G_{7/2}$, are intentionally selected since they meet the approximate condition for proportionality relationship aforementioned. By utilizing the proposed approach, the three JO intensity parameters were obtained ($\Omega_{2,4,6}$ = 12.07, 3.58, and 0.86, respectively, in units of 10^{-20} cm^2). As shown in Table 2, the results determined by our approach are in good agreement with that calculated from the absorption spectrum ($\Omega_{2,4,6}$ = 14.91, 2.19, and 1.30). The value of rmsΔS (0.764 × 10^{-20} cm^2) is within the range for a typical fit to the absorption spectrum.

4.2 YLF:Nd

The proposed approach is also applied to the determination of JO parameters for Nd^{3+} ions in YLF:Nd crystal. Fig. 3 shows the RT excitation and absorption spectra of YLF:Nd powders or crystal. The peak positions and intensities suggest the similarity between the excitation and absorption spectra. It is reasonable to assume that the quantum efficiency of $^4F_{3/2}$ approaches 1, because, considering the maximum phonon energy of the $(LiF_4)^{3-}$ group (about 450 cm^{-1}),[37] at least 12 phonons are required to bridge the large energy gap between $^4F_{3/2}$ and $^4I_{15/2}$ (~5400 cm^{-1}) in YLF:Nd crystal. Therefore the luminescence lifetime of $^4F_{3/2}$ (457 μs) measured by

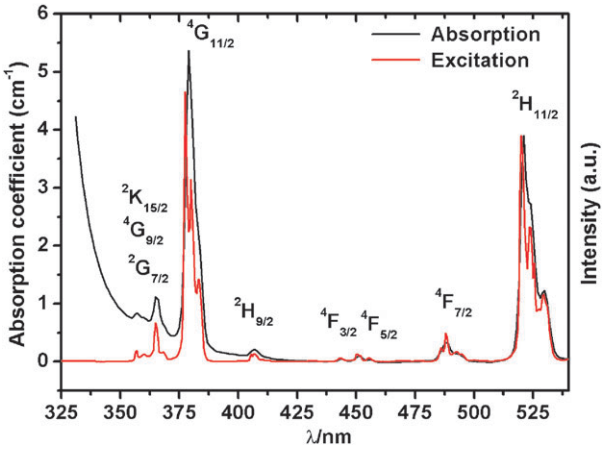

Fig. 2 RT excitation spectrum (red line) of NGW:Er powders by monitoring the Er^{3+} emission at 552 nm. Seven bands labeled in the Figure are chosen for JO intensity calculation. The black line is the unpolarized absorption spectrum of NGW:Er crystal.

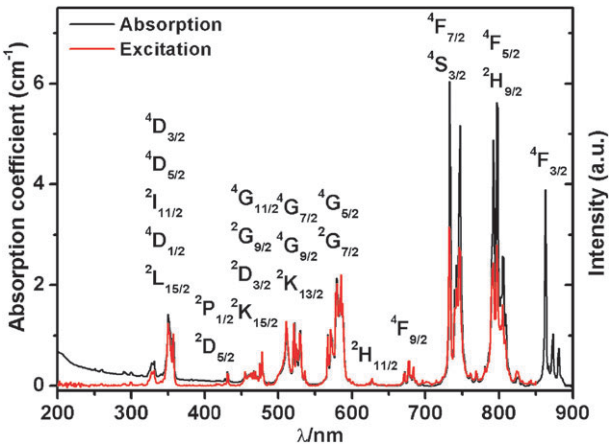

Fig. 3 RT excitation spectrum (red line) of YLF:Nd powders by monitoring the Nd^{3+} emission at 1064 nm. Nine bands labeled in the figure are chosen for JO intensity calculation. The black line is the unpolarized absorption spectrum of YLF:Nd crystal.

Table 2 Comparison of the JO parameters determined from the excitation and absorption spectra (in units of 10^{-20} cm^2)

Samples	Ω_2	Ω_4	Ω_6	rmsΔS	Reference
NGW:Er powder	12.07	3.58	0.86	0.764	This work[a]
NGW:Er crystal	14.91	2.19	1.30	—	34[b]
YLF:Nd powder	0.60	4.91	5.84	0.551	This work[a]
YLF:Nd crystal	0.82	3.08	6.90	0.447	This work[b]
YLF:Nd crystal	0.362	4.02	4.84	0.196	38[b]
Y_2O_3:Er^{3+} nanocrystals	3.58	2.09	0.41	0.185	This work[a]
Y_2O_3:Er^{3+} crystal	4.59	1.21	0.48	—	46[b]

[a] Determined from the excitation spectrum. [b] Determined from the absorption spectrum.

monitoring the RT emission at 1064 nm was approximately regarded as the radiative lifetime in the calculation. Nine excitation bands (Fig. 3) assigned to the multiplets of $^4F_{5/2}$ + $^2H_{9/2}$, $^4F_{7/2}$ + $^4S_{3/2}$, $^4F_{9/2}$, $^2H_{11/2}$, $^4G_{5/2}$ + $^2G_{7/2}$, $^4G_{7/2}$ + $^4G_{9/2}$ + $^2K_{13/2}$, $^4G_{11/2}$ + $^2G_{9/2}$ + $^2D_{3/2}$ + $^2K_{15/2}$, $^2P_{1/2}$ + $^2D_{5/2}$, and $^4D_{3/2}$ + $^4D_{5/2}$ + $^2I_{11/2}$ + $^4D_{1/2}$ + $^2L_{15/2}$ are selected for the determination of JO parameters since they satisfy the approximation assumed in the new approach. As a result, the three JO parameters were obtained ($\Omega_{2,4,6}$ = 0.60, 4.91, and 5.84, respectively, in units of 10^{-20} cm^2). The results derived from the excitation or absorption spectra are compared in Table 2. As shown in Table 2, the Ω_4 calculated from the excitation spectrum (4.91 × 10^{-20} cm^2) are somewhat larger than that from the absorption spectrum (3.08 × 10^{-20} cm^2), whereas $\Omega_{2,6}$ parameters obtained by the two methods vary little. The value of rmsΔS obtained by the excitation spectrum is a little larger than that of the absorption spectrum, which may be due to the fact that more bands in the absorption than in the excitation spectra were involved in the fit of JO parameters. Compared with the parameters $\Omega_{2,4,6}$ (0.362, 4.02, and 4.84, in units of 10^{-20} cm^2) for bulk YLF:Nd crystal reported by Ryan *et al.*,[38] the parameters determined from our approach are slightly larger on the whole. The reason could be that the measured radiative lifetime of $^4F_{3/2}$ (457 μs) adopted in our calculation is smaller than that from Ryan *et al.* (525 μs). If the $^4F_{3/2}$ lifetime of 525 μs were employed in the above calculation, $\Omega_{2,4,6}$ values of 0.53, 4.22, and 5.13 (in units of 10^{-20} cm^2) would be obtained, closer to those reported by Ryan *et al.*

4.3 Y_2O_3:Er^{3+} nanocrystals

The above results reveal that the JO parameters derived from the excitation spectra are basically in accordance with that determined by the commonly used method. To demonstrate its applicability for RE doped nanomaterials, the proposed approach is further employed to determine the JO parameters of Y_2O_3:Er^{3+} (1 at.%) nanocrystals prepared by a sol–gel combustion method. It should be noted that, Er^{3+} doped Y_2O_3 nanocrystals have been extensively studied due to their potential applications in optical communications and biolabels.[39–45] However, to date, no JO parameters are available in the literature to characterize the optical properties of Y_2O_3:Er^{3+} nanocrystals. The phase and morphology of Y_2O_3:Er^{3+} nanoparticles annealed at 850 °C for 2 h were characterized by powder X-ray diffraction (XRD) and TEM experiments. Fig. 4 shows the XRD pattern of the sample. The pattern exhibits well-defined diffraction peaks, indicative of a highly crystallinity of the sample. All the peaks can be exclusively indexed as cubic phase of Y_2O_3 (JCPDS No. 86-1326, space group *Ia-3*). By means of the Debye–Scherrer equation, the average size of Y_2O_3 nanocrystals was estimated to be 53 nm. Fig. 5 shows the TEM (inset) and high resolution TEM images of Y_2O_3:Er^{3+} nanocrystals. As shown in the inset of Fig. 5, the obtained Y_2O_3 nanocrystals were nearly spherical with the mean size of 55 nm, consistent with the value estimated by XRD measurement. The high resolution TEM image revealed very clear crystalline lattice fringes inside a nanoparticle, verifying the very good crystallinity of the sample. The excitation spectrum of Y_2O_3:Er^{3+} was shown in Fig. 6. Similar to NGW:Er, seven bands identified in the RT excitation spectrum by monitoring the emission at 564.0 nm, which correspond to the multiplets of $^2H_{11/2}$, $^4F_{7/2}$, $^4F_{5/2}$, $^4F_{3/2}$, $^2H_{9/2}$, $^4G_{11/2}$, and $^4G_{9/2}$ + $^2K_{15/2}$ + $^2G_{7/2}$, are selected as target multiplets in the calculation. The wavelength-dependent refractive index, *n*, of cubic Y_2O_3 was derived from the Cauchy

formula, $n(\lambda) = 1.780 + 0.01598\cdot\lambda^{-2}$.[46] For Y_2O_3 nanocrystals, the effective index of refraction can be expressed as: $n_{eff} = n(\lambda)_{Y2O3}\cdot x + (1 - x)\cdot n_{med}$, where $n(\lambda)_{Y2O3}$ is the refractive index of Y_2O_3 (1.805 at the wavelength of 1535.4 nm). To determine the filling factor x, we measured the $^4I_{13/2}$ lifetimes of Er^{3+} in Y_2O_3 nanocrystals being immersed in solvents with different refractive indices. The media included air ($n = 1$), ethanol (CH_3CH_2OH, $n = 1.361$), methylbenzene ($C_6H_5CH_3$, $n = 1.497$) and carbon disulfide (CS_2, $n = 1.628$). Although the refractive indices of solvents or air in which Y_2O_3 nanocrystals were immersed vary from 1.0 to 1.63, numerical calculations show that the ratio of χ_{ED} to χ_{MD} can be well approximated to be 1. As shown in Fig. 7a, such approximation is accurate to within $\sim$10% for n_{med} in a range from 1.0 to 2.2. In view of the intrinsic accuracy of JO parameters calculation (usually within 10–20%), it is reasonable to assume that χ_{ED} equals to χ_{MD} in this case. Particularly, for the $^4I_{13/2} \rightarrow {}^4I_{15/2}$ transition, eqn (3) can thus be simplified as:

$$\tau_r(^4I_{13/2})^{-1} \approx \frac{64\pi^4 e^2}{3h(2J+1)\bar{\lambda}^3}\chi_{ED}\cdot \left[\sum_{t=2,4,6}\Omega_t|\langle\Phi J||U^{(t)}||\Phi' J'\rangle|^2 + |\langle\Phi J||M||\Phi' J'\rangle|^2\right] \quad (6)$$

Two macroscopic models have recently been proposed for the dependence of the radiative relaxation probability of luminescent centers embedded in surrounding media with various refractive indexes, *i.e.* the virtual-cavity model and the real-cavity model.[47,48] In this case, the virtual-cavity model was used to simulate the dependence of $^4I_{13/2}$ lifetime of Er^{3+} in Y_2O_3 nanocrystals on the refractive indexes of the surrounding media with $\chi_{ED} = n_{eff}(n_{eff}^2 + 2)^2/9$ in eqn (6). Fig. 7b shows the dependence of the observed $^4I_{13/2}$ lifetime of Er^{3+} in Y_2O_3 nanocrystals on the refractive index of the media at RT. Using x as an adjustable parameter, the experimental data were fitted with eqn (6) and a filling factor of 87% yielded an optimal fit. In order to compare our results with the

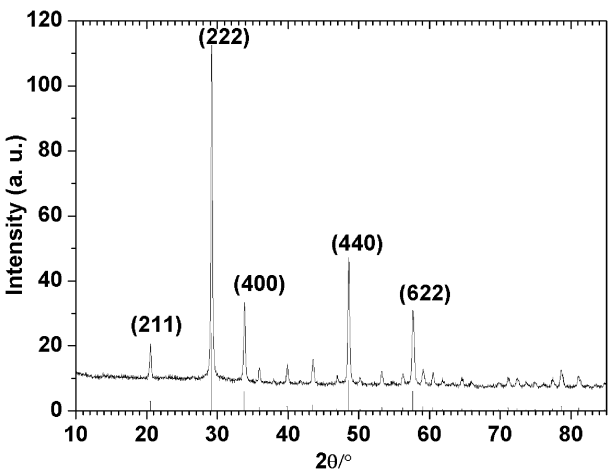

Fig. 4 XRD pattern of $Y_2O_3:Er^{3+}$ nanocrystals, the vertical lines represent the standard data of cubic phase Y_2O_3 (JCPDS No. 86-1326, space group *Ia-3*).

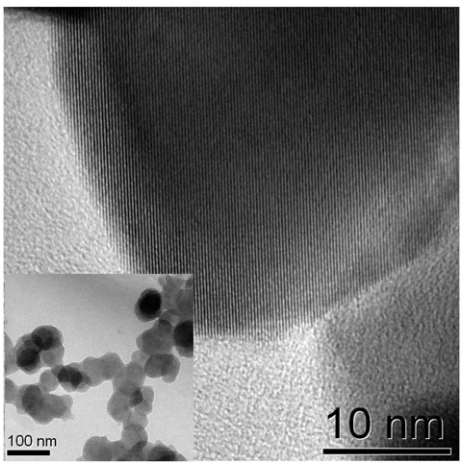

Fig. 5 TEM image (inset) and high resolution TEM image of $Y_2O_3:Er^{3+}$ nanocrystals.

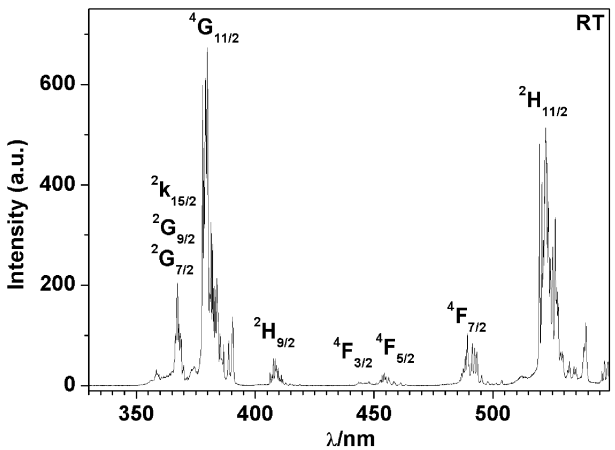

Fig. 6 RT excitation spectrum of Er^{3+} doped Y_2O_3 nanocrystals by monitoring the Er^{3+} emission at 564.0 nm. Seven bands assigned in the Figure are chosen for JO intensity calculation.

JO parameters of $Y_2O_3:Er^{3+}$ bulk crystals,[46] the same sets of RMEs of the unit tensor for the ED and the MD transitions were used in our calculation.[33,49] By a least-squares fitting of S_{cal} to the measured line strength S_{mea}, the ratios of the three JO intensity parameters were obtained. Subsequently, by subtracting the MD contribution on the $^4I_{13/2} \rightarrow {}^4I_{15/2}$ transition from the total radiative transition rate, the obtained ED radiative transition rate of $^4I_{13/2}$ was used as a standard to determine the absolute values of $\Omega_{2,4,6}$ parameters. It should be noted that the influence of the cross-relaxation process of the neighboring Er^{3+} ions on the luminescence lifetime should also be considered. To minimize the effect of concentration quenching on the fluorescence kinetics, the decay of $^4I_{13/2}$ in $Y_2O_3:Er^{3+}$ nanocrystals with much lower dopant concentration (0.5 at.%) was measured, which showed the same decay time as that of the 1at.% Er^{3+} doped sample. Thus the Er–Er cross-relaxation process can be neglected in this case. The experimental radiative lifetime of $^4I_{13/2}$ of Er^{3+} in Y_2O_3 nanocrystals was measured to be 8.24 ms by monitoring the emission of $^4I_{13/2} \rightarrow {}^4I_{15/2}$ at 1535.4 nm. The obtained lifetime is close to that of Er^{3+} in Y_2O_3 bulk crystal.[46] It should be

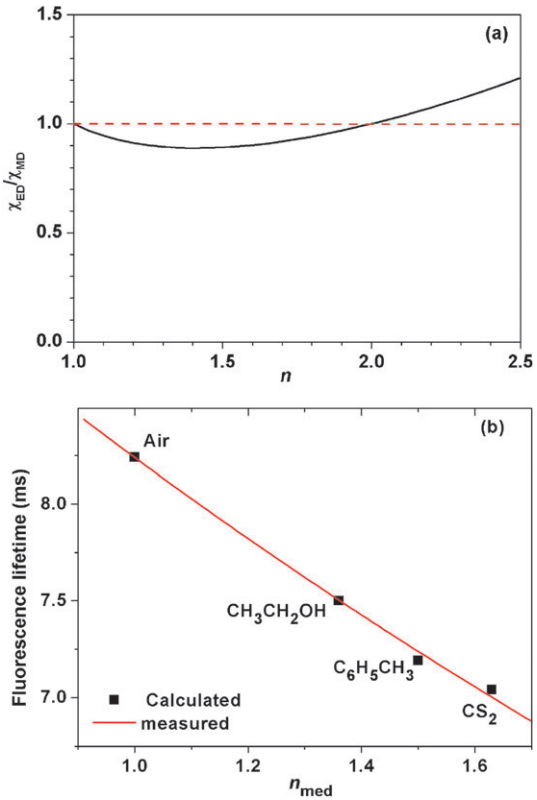

Fig. 7 (a) The plot of the ratio χ_{ED}/χ_{MD} *versus* the refractive index *n*. (b) Dependence of the $^4I_{13/2}$ lifetime of Er^{3+} in Y_2O_3 nanocrystals on the refractive index of the surrounding medium (n_{med}).

mentioned that the anomalously long lifetime of $^4I_{13/2}$ (48 ms) for Y_2O_3:Er^{3+} nanocrystals recently reported by Sardar *et al.*[50] remains very suspicious because it is more than six times the radiative lifetime (7.75 ms) reported by Weber.[46] As a result, the three JO intensity parameters were obtained ($\Omega_{2,4,6}$ = 3.58, 2.09 and 0.41, in the units of 10^{-20} cm^2). In principle, compared to the bulk crystal, the particle size (or quantum confinement) should have little impact on the JO parameters for RE-doped insulator nanocrystals with a size larger than 10 nm. In contrast to the JO parameters ($\Omega_{2,4,6}$ = 4.59, 1.21 and 0.48) for Y_2O_3:Er^{3+} bulk crystal,[46] Ω_6 varied little, whereas Ω_2 is somewhat smaller and Ω_4 is larger than the Y_2O_3:Er^{3+} crystal. Nevertheless, the determined JO parameters are comparable to those bulk values. For comparison, we performed the above fit for the case not considering the correction of effective refractive index for nanocrystals (namely, assuming a filling factor of 100%). The fitting resulted in the values ($\Omega_{2,4,6}$ = 3.08, 1.81 and 0.36, in the units of 10^{-20} cm^2), which are smaller on the whole than that when considering the refractive index correction and deviate more from the bulk values.

Finally, it is worth re-emphasizing that the method we proposed is based on a prerequisite that a very fast nonradiative de-excitation/relaxation to the monitored level occurs for the excited levels involved in the fitting. Obviously, long-lived metastable excited states are not suitable for this method, such as the $^4S_{3/2}$, $^4F_{9/2}$ and $^4I_{9/2}$ multiplets of Er^{3+} when monitoring the emission from $^4I_{13/2}$, since radiative de-excitations may occur between them. Besides, those hosts with lower maximum phonon energy could be ideal systems for the application of the proposed approach, since the multi-phonon nonradiative transition from the metastable state can be significantly inhibited. Consequently the measured lifetime from the metastable level can be approximately regarded as its radiative lifetime, which is used to determine the absolute values of JO parameters.

Conclusions

In summary, a new method based on the measurement of the excitation spectrum for RE doped powder or nanocrystalline materials is proposed to determine the JO intensity parameters, which are useful in evaluating the spectral properties of RE^{3+} ions in a series of luminescent materials. The approach has been successfully applied to three systems: NGW:Er powders, YLF:Nd powders, and Y_2O_3:Er^{3+} nanocrystals. The JO parameters determined from this approach are in good agreement with that determined from the conventional method. This approach is particularly valuable for those powders or nano-phosphors that their quantitative absorption spectra are difficult to measure.

Acknowledgements

This work is supported by the Hundreds of Talents and Knowledge Innovation Programs of the Chinese Academy of Sciences (CAS) for Key Topics (No. KJCX2-YW-358) and Young Scientists, Instrument Developing Project of CAS (No. YZ200712), the NSFC (Nos. 10774143, 10804106 and 10974200), the 973 and 863 programs of MOST (Nos. 2007CB936703 and 2009AA03Z430), Fujian Provincial Science Fund for Distinguished Young Scholars (No. 2009J06030), and the Key Project of Science and Technology Foundation of Fujian Province (Nos. 2007I0024 and 2007HZ005-3). We thank Fujian Castech Crystals, INC and Prof. Yidong Huang for kindly providing us the YLF:Nd and NGW:Er crystals.

Notes and references

1 S. Comby, J.-C. G. Bünzli, V. K. Pecharsky, J.-C. G. Bünzli and K. A. J. Gschneider, in *Handbook on the Physics and Chemistry of Rare Earths*, ed. V. K. Pecharsky, J.-C. G. Bünzli and K. A. Gschneider, Jr., Elsevier, 2007, vol. 37, p. 217.
2 J. C. Boyer, F. Vetrone, L. A. Cuccia and J. A. Capobianco, *J. Am. Chem. Soc.*, 2006, **128**, 7444.
3 J. C. Boyer, L. A. Cuccia and J. A. Capobianco, *Nano Lett.*, 2007, **7**, 847.
4 J. C. G. Bunzli and C. Piguet, *Chem. Soc. Rev.*, 2005, **34**, 1048.
5 J. C. G. Bunzli, *Acc. Chem. Res.*, 2006, **39**, 53.
6 F. Wang and X. G. Liu, *Chem. Soc. Rev.*, 2009, **38**, 976.
7 J. C. Boyer, N. J. J. Johnson and F. C. J. M. van Veggel, *Chem. Mater.*, 2009, **21**, 2010.
8 S. Sivakumar, F. C. J. M. van Veggel and P. S. May, *J. Am. Chem. Soc.*, 2007, **129**, 620.
9 S. Sivakumar, F. C. J. M. van Veggel and M. Raudsepp, *J. Am. Chem. Soc.*, 2005, **127**, 12464.
10 J. W. Stouwdam and F. C. J. M. van Veggel, *Nano Lett.*, 2002, **2**, 733.
11 L. Y. Wang, R. X. Yan, Z. Y. Hao, L. Wang, J. H. Zeng, H. Bao, X. Wang, Q. Peng and Y. D. Li, *Angew. Chem., Int. Ed.*, 2005, **44**, 6054.

12 P. Li, Q. Peng and Y. D. Li, *Adv. Mater.*, 2009, **21**, 1945.
13 H. X. Mai, Y. W. Zhang, R. Si, Z. G. Yan, L. D. Sun, L. P. You and C. H. Yan, *J. Am. Chem. Soc.*, 2006, **128**, 6426.
14 R. Si, Y. W. Zhang, L. P. You and C. H. Yan, *Angew. Chem., Int. Ed.*, 2005, **44**, 3256.
15 B. M. van der Ende, L. Aarts and A. Meijerink, *Adv. Mater.*, 2009, **21**, 3073.
16 F. Vetrone, R. Naccache, V. Mahalingam, C. G. Morgan and J. A. Capobianco, *Adv. Funct. Mater.*, 2009, **19**, 2924.
17 V. Mahalingam, F. Vetrone, R. Naccache, A. Speghini and J. A. Capobianco, *Adv. Mater.*, 2009, **21**, 4025.
18 B. R. Judd, *Phys. Rev.*, 1962, **127**, 750.
19 G. S. Ofelt, *J. Chem. Phys.*, 1962, **37**, 511.
20 C. Gorller-Warland and K. Binnemans, in *Handbook on the Physics and Chemistry of the Rare Earths*, ed. K. A. Gschneidner, Jr. and L. Eyring, North-Holland, Amsterdam, 1998, vol. 25, p. 101.
21 W. F. Krupke, *Phys. Rev.*, 1966, **145**, 325.
22 J. C. Boyer, F. Vetrone, J. A. Capobianco, A. Speghini and M. Bettinelli, *J. Phys. Chem. B*, 2004, **108**, 20137.
23 Y. S. Liu, W. Q. Luo, R. F. Li, G. K. Liu, M. R. Antonio and X. Y. Chen, *J. Phys. Chem. C*, 2008, **112**, 686.
24 J. Sytsma, G. F. Imbusch and G. Glasse, *J. Chem. Phys.*, 1989, **91**, 1456.
25 M. G. King, *Appl. Opt.*, 1975, **14**, 1627.
26 X. Y. Chen, M. P. Jensen and G. K. Liu, *J. Phys. Chem.B*, 2005, **109**, 13991.
27 X. Y. Chen, E. Ma and G. K. Liu, *J. Phys. Chem. C*, 2007, **111**, 10404.
28 W. D. Partlow and H. W. Moos, *Phys. Rev.*, 1967, **157**, 252.
29 R. S. Meltzer, S. P. Feofilov, B. Tissue and H. B. Yuan, *Phys. Rev. B: Condens. Matter Mater. Phys.*, 1999, **60**, R14012.
30 W. F. Krupke, *IEEE J. Quantum Electron.*, 1971, **7**, 153.
31 W. T. Carnall, H. Crosswhite and H. M. Crosswhite, *Energy Level Structure and Transition Probabilities in the Spectra of the Trivalent Lanthanides in Lanthanum Fluoride*, Argonne National Laboratory Report, Argonne, IL, USA, 1978.
32 Z. D. Luo, Y. D. Huang and X. Y. Chen, *Spectroscopy of Solid-State Laser and Luminescent Materials*, Nova Science Publishers, New York, 2007.
33 M. J. Weber, *Phys. Rev.*, 1967, **157**, 262.
34 J. H. Huang, X. H. Gong, Y. J. Chen, Y. F. Lin, J. S. Liao, X. Y. Chen, Z. D. Luo and Y. D. Huang, *Appl. Phys. B: Lasers Opt.*, 2007, **89**, 73.
35 J. Hanuza, L. Macalik and A. A. Kaminskii, *J. Mol. Struct.*, 2000, **555**, 289.
36 M. C. Pujol, M. A. Bursukova, F. Guell, X. Mateos, R. Sole, J. Gavalda, M. Aguilo, J. Massons and F. Diaz, *Phys. Rev. B: Condens. Matter Mater. Phys.*, 2002, **65**, 165121.
37 E. S. Y. S. Raptis, E. Zouboulis and C. Raptis, *Phys. Rev. B: Condens. Matter Mater. Phys.*, 1999, **59**, 4154.
38 J. R. Ryan and R. Beach, *J. Opt. Soc. Am. B*, 1992, **9**, 1883.
39 P. A. Tanner and K. L. Wong, *J. Phys. Chem. B*, 2004, **108**, 136.
40 J. A. Capobianco, F. Vetrone, T. D'Alesio, G. Tessari, A. Speghini and M. Bettinelli, *Phys. Chem. Chem. Phys.*, 2000, **2**, 3203.
41 Y. B. Mao, T. Tran, X. Guo, J. Y. Huang, C. K. Shih, K. L. Wang and J. P. Chang, *Adv. Funct. Mater.*, 2009, **19**, 748.
42 J. A. Capobianco, F. Vetrone, J. C. Boyer, A. Speghini and M. Bettinelli, *J. Phys. Chem. B*, 2002, **106**, 1181.
43 F. Vetrone, J. C. Boyer, J. A. Capobianco, A. Speghini and M. Bettinelli, *Chem. Mater.*, 2003, **15**, 2737.
44 F. Vetrone, J. C. Boyer, J. A. Capobianco, A. Speghini and M. Bettinelli, *J. Phys. Chem. B*, 2003, **107**, 1107.
45 F. Vetrone, J. C. Boyer, J. A. Capobianco, A. Speghini and M. Bettinelli, *J. Appl. Phys.*, 2004, **96**, 661.
46 M. J. Weber, *Phys. Rev.*, 1968, **171**, 283.
47 C. K. Duan and M. F. Reid, *Spectrosc. Lett.*, 2007, **40**, 237.
48 C. K. Duan, M. F. Reid and Z. Q. Wang, *Phys. Lett. A*, 2005, **343**, 474.
49 W. T. Carnall, P. R. Fields and B. G. Wybourne, *J. Chem. Phys.*, 1965, **42**, 3797.
50 D. K. Sardar, K. L. Nash, R. M. Yow and J. B. Gruber, *J. Appl. Phys.*, 2007, **101**, 113115.

